Applied Geochemistry 100 (2019) 203–212

Contents lists available at ScienceDirect

Applied Geochemistry

journal homepage: www.elsevier.com/locate/apgeochem

The geochemistry and origin of fluids in the carbonate structure of the Hranice Karst with the world's deepest flooded cave of the Hranicka Abyss, Czech Republic

O. Sracek[a,*], M. Geršl[b], J. Faimon[a], O. Bábek[a]

[a] Department of Geology, Faculty of Science, Palacky University, 17. listopadu 12, 771 46, Olomouc, Czech Republic
[b] Department of Agricultural, Food and Environmental Engineering, Mendel University, Zemědělská 1, 613 00, Brno, Czech Republic

ARTICLE INFO

Editorial handling by Dr F Chabaux

Keywords:
Carbonate aquifer
Recharge
Endogenic CO_2
Carbon isotope modeling
Hranicka abyss

ABSTRACT

The origin of fluids in the Hranice Karst containing the deepest flooded abyss in the world has been investigated using hydrogeological, hydrogeochemical, and isotopic data. At least a part of the CO_2 gas originates in the mantle as indicated by very enriched $\delta^{13}C$(DIC) values and from existing He isotope analyses. The origin of groundwater in the karstic aquifer which is exploited at the Teplice nad Bečvou Spa is meteoric with a recharge area about 200 m above the Bečva River valley as indicated by depleted values of $\delta^{2}H$ and $\delta^{18}O$ compared to the river water. Based on detectable tritium, the groundwater is from 20 to 50 years old. Water in the Hranicka Abyss and in the Zbrašov Aragonite Caves is a mixture of carbonate aquifer groundwater with the river and/or shallow groundwater comprising variable proportions of both end-members. Water in Death Cave Lake seems to be affected by agriculture contaminated shallow groundwater as indicated by increased nitrate concentration. Inverse geochemical modeling of aquifer geochemistry suggested two scenarios: (1) reaction of Mg-rich calcite with deep hypogenic CO_2 (about 30 mmol/l) plus dissolution of trace amounts of halite and sylvite and cation exchange; (2) reaction of Mg-depleted calcite and Mg-silicate (talc) as a source of Mg together with deep CO_2. Both scenarios were calibrated using $\delta^{13}C$(DIC) values and gave satisfactory results. A conceptual model of the site has been developed which includes a gravity-driven flow system where meteoric water which has recharged in the surrounding uplands is heated at depth and acquires large amounts of hypogenic CO_2, which preferentially dissolves Mg-carbonates along the pre-existing tectonic features. The Miocene transgression followed by the later incision of the Bečva Valley played an important role in groundwater circulation and the origin of fluids.

1. Introduction

Carbonated mineral/thermal waters represent water saturated by gaseous CO_2 under enhanced hydrostatic pressure. Specific geological conditions are required for their formation, such as deep tectonics in the crust, which provides a supply of juvenile carbon dioxide. Generation of these fluids is often related to the presence of deep tectonic faults from the crust to upper mantle (reaching depths of 25–30 km is not extraordinary). Three principal sources of endogenic CO_2 can be identified in such waters: transformation of organic matter during the formation of fossil coal, oil and gas, metamorphic transformation of carbonates, and de-gassing associated with volcanic activities (Goldscheider et al., 2010). Generally, endogenous CO_2 moves upward at the intersection of several faults where the CO_2 comes into contact with groundwater in which it dissolves (Weinlich et al., 1999). This creates carbonic acid that aggressively attacks rocks (e.g., with rocks containing carbonates such as limestone, dolomite, or calcareous sandstone). Under favorable conditions, hypogenic karst can develop where karstification proceeds upward, with resulting complex karst structures (Audra and Palmer, 2015), e.g. in Buda, Hungary (Goldscheider et al., 2010; Havril et al., 2016), Italy (Minissale et al. (2002), or Jordan (Bajjali et al., 1997). There are several types of hypogenic karst, e.g. karst linked to CO_2 or hydrogen sulphide, although the latter type is much less common. Where large inputs of endogenic CO_2 and favorable tectonic setting are found, deep flooded abyss and sinkhole structures can develop, e.g. Sistema Zacatón in Mexico (Gary and Sharp, 2006) and Pozzo del Merro in Italy (Caramana, 2002). Groundwater in hypogenic karst is generally of meteoric origin. Surface water is driven to depth by high topographic gradients between elevated recharge zones and lower discharge zones with resulting high hydraulic gradients (Tóth, 1999). Modeling of hypogenic karst development (Mádl-Szönyi and Tóth, 2015; Havril et al., 2016) has provided

* Corresponding author. Department of Geology, Faculty of Science, Palacky University, 17. listopadu 12, 771 46, Olomouc, Czech Republic.
E-mail address: srondra@seznam.cz (O. Sracek).

https://doi.org/10.1016/j.apgeochem.2018.11.013
Received 31 July 2018; Received in revised form 16 November 2018; Accepted 18 November 2018
Available online 22 November 2018
0883-2927/

insight into the origin of hypogenic karst. In an initial confined state of a karstic aquifer thermal convection cells can develop with buoyancy-driven flow. In later stages, when the confining layer is partly eroded and recharge and discharge areas develop due to tectonic uplift and river incision, these cells are overprinted by advective gravity-driven flow. Karst development then accelerates caused by penetration of recharge water into a karst system. When groundwater ascends towards discharge areas, it cools down, dissolves carbonates and enlarges existing fractures (Andre and Rajaram, 2004; Sandeep et al., 2016). Genesis of hypogenic caves has been reviewed by Klimchouk (2009), who stressed the importance of permeability structures in cave formation, including the discordance of permeability between karst aquifers and adjacent confining layers. An example of hypogenic caves which developed under confined conditions by rising flow are Toca da Boa Vista and Toca da Barriguda in Precambrian carbonates in Bahia State in northeastern Brazil (Klimchouk et al., 2016).

The Nysa-Morava Zone (NMZ) at the northeastern margin of the Bohemian Massif, rich in mineral water manifestations, represents a prominent strike-slip tectonic domain governed by deep-seated, NW-SE trending faults of the Elbe Fault Zone. Its late Miocene to present-day evolution is largely governed by the thrust-and-sheet tectonic style of the overriding Western Carpathians (Špaček et al., 2015). The studied Hranice Karst is located in the eastern central part of the NMZ, close to the town of Teplice nad Bečvou on the Bečva River (Fig. 1). Typical karst structures are the Zbrašov Aragonite Caves and, in particular, the Hranicka Abyss, which is currently (2018) the deepest flooded abyss in the world. The karst has developed in the Devonian carbonates and the input of endogenous CO_2 results in the formation of sparkling waters which are exploited in the Teplice nad Bečvou spa for balneological purposes.

The objectives of this study were to determine (1) the origin of fluids in this hypogenic karst structure, and (2) the recharge zone of the carbonate aquifer, exploited in the spa.

2. Site geology and hydrogeology

The hypogenic karst is found in a small outcrop (~5 x ~3 km) of Devonian to Mississippian carbonates located in the eastern part of the Czech Republic (N 49°31′, E 17°45′), at the contact between the eastern Bohemian Massif and the Outer Western Carpathians. The study area (Fig. 1) constitutes a part of the Palaeozoic sedimentary cover of the Brunovistulian unit, which was deformed during the Variscan orogeny (Kalvoda et al., 2008). The Brunovistulian basement is composed of upper Proterozoic high- and medium-grade metamorphic acid igneous rocks and metasediments of the Brunovistulian unit recycled during the Variscan orogeny. This crystalline basement is covered by a Middle Devonian (Eifelian) to Mississippian (Viséan) clastic-carbonate sedimentary succession reaching an aggregate thickness of up to 7 km (Schulmann and Gayer, 2000; Hartley and Otava, 2001; Kalvoda et al., 2008). The karstification is developed in Givetian to Tournaisian fossiliferous, crinoidal and coral-stromatoporoid floatstones and wacke/packstones, pelagic nodular wacke/packstones and intraclastic carbonate breccias of the Macocha and Líšeň Formation (Dvořák and Friáková, 1978). A part of the carbonate succession was overprinted by late Variscan penetrative foliation, which largely controls the morphology of the karst. The thickness of the carbonate succession is unknown in the study area, however in the Chorynĕ-9 drillhole located 11.5 km SE, it reaches ~1200 m. The Palaeozoic rocks are deformed into a thin-skinned stack of thrust sheets separated by N/NW-dipping thrust faults (Čížek and Tomek, 1991). The Palaeozoic rocks are overlain by a succession of Miocene shallow-marine deposits of the Carpathian Foredeep. Following a long period of denudation in non-marine environment, the area was affected by Middle Miocene (early Langhian) transgression of the Carpathian Foredeep, associated with deposition of siliciclastic sandstones, conglomerates, mixed with shallow-water carbonates with abundant bryozoans, red algae, bivalves and foraminifers (Kováč et al., 2007; Holcová et al., 2015). This sequence passes laterally to more deep-water calcareous mudstones with abundant planktonic and benthic foraminifers, diatoms, ostracods and radiolarians. However, before the transgression, the Palaeozoic carbonates were located above sea level and developed distinct karst morphology, as evidenced from geophysical surveying of the buried pre-Miocene surface in the vicinity of Hranice (Tyráček, 1962; Dleštík and Bábek, 2013), from Miocene Neptunian dykes and traces of bivalve borings found in the Palaeozoic carbonates. In addition, the Miocene calcareous siliciclastics are exposed in the dry parts of the Hranická Abyss indicating that the abyss itself was open already before the Miocene transgression. The entire area is covered by Quaternary loess and colluvial deposits.

The tectonic structure of the area and morphology of the hypogenic karst was strongly affected by the Oligocene-Miocene thrusting of the Western Carpathians. In response to the thrusting, the foreland of the eastern Bohemian Massif developed a distinct late Cenozoic structure of the Nysa-Morava Zone (NMZ) at the intersection between the SW-NE trending Carpathian thrust sheets and the SE-NW trending Elbe Fault Zone (Špaček et al., 2015). The NMZ is characterized by SE-NW trending geomorphic faults and numerous carbonate springs bound to the deep-seated faults (Špaček et al., 2015). The faulting is associated with Plio-Pleistocene alkali basic volcanism (Ulrych et al., 2013), evidence of historical and paleoseismic events (Guterch and Lewandowska-Marciniak, 2002; Bábek et al., 2015), present-day seismicity, and development of horst-and-graben basins filled with Pliocene and Quaternary clastic sediments (Novák et al., 2017).

A carbonate aquifer is exploited at the Teplice nad Bečvou spa, with two pumping wells 60.4 m and 101.8 m deep (Fig. 1). As previously mentioned, one of the most significant associated hydrologic and geomorphic phenomena is the Hranicka Abyss, which is currently the deepest underwater cave in the world with a possible depth of 700–800 m (e.g., Bunta, 2015). The Hranicka Abyss is filled with carbonated mineral water of largely unknown origin. However, given its geological framework at the contact between the Bohemian Massif and Western Carpathians, the formation of the abyss as well as the surrounding mineral springs is assumed to be associated with the supply of juvenile CO_2 from deeper crustal parts (Špaček et al., 2015). An unconfined or perched aquifer might exist in the uplands above the river valley, but boreholes drilled in the region for construction purposes were dry and no water chemistry data are available.

3. Material and methods

Ground water was sampled from two pumping wells in the spa, while karst water was sampled from two underground lakes in the Zbrašov Aragonite Caves, from Death Cave (DC) and from B Cave (BC), and from the Hranicka Abyss (HA), and river water was sampled in the Bečva River (BR) upstream of the spa (Fig. 1). Temperature, pH and electrical conductivity (EC) were measured on-site. The samples for cation and trace element analyses were pre-filtered with 0.45 mm Millipore filters, acidified with HNO_3-Suprapur, stored in HDPE bottles, and analyzed with the ICP-MS technique. The analytical precision of the individual solution analyses was below 2%. Anions were determined by HPLC (Dionex ICS, 2000). Alkalinity was determined by titration with HCl using the Gran plot to determine the end point. All charge balance errors were in the range ± 5%.

Isotope values for δ^2H and $\delta^{18}O$ in water were determined at the Czech Geological Survey in Prague using a LWIA 3000 laser analyzer (LGR). Precision was 0.4‰ for δ^2H and 0.12‰ for $\delta^{18}O$. The results were normalized to the internationally accepted standard (V-SMOW) and reported in the usual δ-notation.

For the ^{13}C analyses, $BaCl_2$ was added and then pH was increased to about 12 by NaOH. The $BaCO_3$ precipitate was used for $\delta^{13}C$(DIC) determination. The precipitate was decomposed in 100% H_3PO_4 in a vacuum at 25 °C. The C isotopes in the generated CO_2 were determined by a Thermo Delta V isotope ratio mass spectrometer with precision of

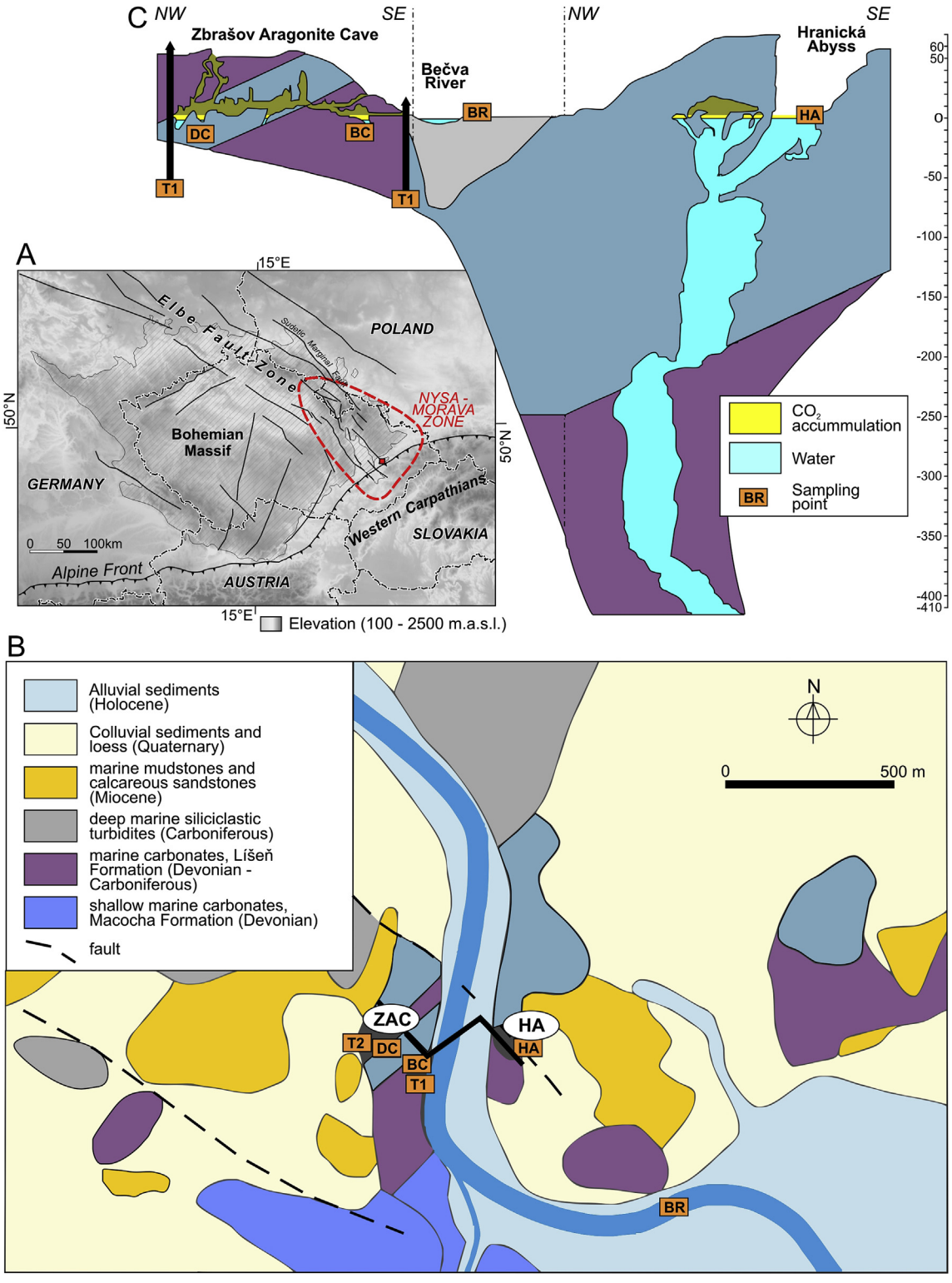

Fig. 1. (a) Location of the study site, (b) geological map, (c) cross-section illustrating the principal tectonic and karstic features in study area. ZAC-Zbrašov Aragonite Caves, HA-Hranicka Abyss, T1,T2-pumping wells, DC-Death Cave, BC-B Cave, BR-Bečva River.

$\delta^{13}C$ better than 0.1‰. Results were expressed with respect to the PDB standard. Sulfate sulfur from waters was precipitated with $BaCl_2$ as $BaSO_4$, mixed with V_2O_5 and silica and decomposed in a vacuum under a temperature of 1050 °C. Produced SO_2 was stored in glass ampules for measurement. Reproducibility was ± 0.3‰. Calibration of the laboratory standard was carried out by the IAEA international standards (NBS122 and NBS127).

Measurements of ^3H were performed at the Institute of Nuclear Research in Řež by a TriCarb 3170TR/SL apparatus. Samples for ^3H analyses were enriched by electrolysis in a solution of Na_2O_2 and each sample was measured 4 times for a period of 700 min.

Data on helium isotopes based on a previous project were taken from the literature (Meyberg and Rinne, 1995) and interpreted together with isotopic data acquired in this study.

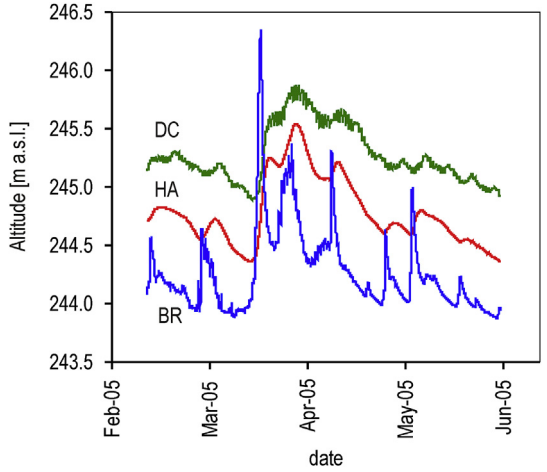

Fig. 2. Water level data for the Bečva River (BR), Hranicka Abyss (HA), and Death Cave (DC) between February 2005 and June 2005.

The program PHREEQC (Parkhurst and Appelo, 1999) was used to calculate speciation and to model mass transfer using the inverse geochemical modeling module. Multivariate statistics was performed using the STATISTICA program, version 7.1. (Statsoft Inc., 2005). Data on chemical composition were recalculated into mmol/l units. After the Centered Log-Ratio Transformation (Aitchison, 1986; Davies, 2002; Filzmoser et al., 2009), the data were subjected to Hierarchic Cluster Analysis (HCA).

4. Results

4.1. Water level data

Based on water level data (Fig. 2), the water level in the Hranicka Abyss (HA) in the study period is generally higher (average value of 244.51 m ASL) than in the river (BR) (average value of 244.12 m ASL) and the expected flow direction is towards the river. However, the situation is complicated by a two-phase regime and resulting lower density of water in the abyss. Also, the HA has a constant temperature of 15 °C, which is higher than the river water temperature for most of year. Hydraulic head data in the HA and DC corrected for the same water density are therefore probably at similar levels as in the river except during extreme flood events in the river such as in March 2005. The water level data in Death Cave are affected by the pumping of groundwater in wells T1 and T2 in the spa. In summary, it seems that during most of year there is flow from the karst caves and the abyss towards the river, or there is only limited exchange due to hydrodynamic equilibrium, but reversed flow can occur during extreme water levels in the river.

4.2. Water chemistry data

Water chemistry data for selected sampling points and sampling in May 2017 are provided in Table 1 and they are also plotted in a Piper diagram in Fig. 3. We consider the data as representative because there are no significant temporal changes in water chemistry (Geršl, 2016).

Groundwater in the carbonate aquifer (T1, T2), Hranicka Abyss (HA), and the B Cave have Ca^{2+} concentrations of about 500 mg/l and HCO_3^- concentrations up to 1900 mg/l. In contrast, concentrations in Death Cave and especially in the river are much lower. Water in Death Cave also has increased concentrations of NO_3^- and Cl^-, suggesting input from the shallow contaminated aquifer. Concentrations of Na^+ and Mg^{2+} are much lower, always below 100 mg/l.

Based on the Piper diagram (Fig. 3), all waters are of the Ca-HCO_3 type. Their principal differences are in Ca and alkalinity/HCO_3 concentrations.

Table 1
Water chemistry data.

Sample/ parameter	T1	T2	Hranická Abyss (HA)	Bečva River (BR)	B Cave (BC)	Death Cave (DC)
T [°C]	24	22.5	16.8	15.7	21	23
pH	6.31	6.28	6.27	7.81	6.44	6.58
Eh [mV]	293	270	385	412	373	375
EC [mS/cm]	2.785	2.805	2.459	0.428	2.75	1.60
K [mg/l]	13.1	12.3	8.4	6.9	11.4	6.4
Na [mg/l]	92	83	55	17	87	34
Ca [mg/l]	494	490	426	58	516	316
Mg [mg/l]	58	51	38	8.8	55	20
HCO_3 [mg/l]	1894	1827	1413.7	172.3	1877.3	982
SO_4 [mg/l]	23.9	26.4	67.8	39.3	23.9	68.7
Cl [mg/l]	28.1	32.6	55.3	14.8	32.5	55.1
F [mg/l]	2.02	2.11	1.36	0.16	2.20	0.57
NO_3 [mg/l]	0.24	0.38	1.45	8.8	1.45	17.5
Si [mg/l]	10.2	10.4	7.6	1.3	10.3	8.1
Fe [mg/l]	0.061	0.041	0.81	0.005	0.027	0.012
Mn [mg/l]	0.245	0.356	0.203	0.011	0.231	0.009
Li [μg/l]	93.78	90.64	55.18	6.048	100.4	21.58
Be [μg/l]	0.502	0.492	0.383	0.02	0.524	0.063
Ti [μg/l]	11.97	13.09	25.32	1.17	13.59	9.938
Cr [μg/l]	23.0	26.42	121.2	37.74	26.69	53.26
Ni[μg/l]	28.23	25.95	21.51	3.858	27.33	15.28
Cu [μg/l]	7.897	1.607	2.134	2.694	0.510	1.908
Zn [μg/l]	1.867	2.504	2.986	0.541	2.568	26.66
Rb [μg/l]	31.12	29.36	18.99	1.194	30.67	7.033
Cs [μg/l]	5.352	5.331	2.888	0.042	5.205	3.43
Sr [μg/l]	2039	1945	1299	363.6	1978	649.3
Ba [μg/l]	1001	938.3	480.1	62.34	887.3	81.3
Th [μg/l]	0.003	0.001	0.042	0.001	0.001	0.001
U [μg/l]	0.517	0.531	0.785	0.18	0.501	0.946

4.3. Isotopic data

Isotopic data are shown in Table 2. Data for δ^2H and $\delta^{18}O$ isotopes are plotted in Fig. 4 and $\delta^{13}C$ vs HCO_3 is plotted in Fig. 5.

In Fig. 4, there is no impact of evaporation on the δ^2H and $\delta^{18}O$ isotope data, indicating relatively fast infiltration. Surface water in the Bečva River (BR) has generally constant values, which are enriched compared to other samples. The exception is sample BR-3 from February 2018 with more depleted values which were comparable to the HA value. The sampling was performed after a cold spell with snowfall thus these values are probably caused by melting of snow at higher altitudes of the catchment. Water from the carbonate aquifer (T1 and T2) is isotopically depleted compared to river water, suggesting a higher altitude of the recharge zone compared to the river altitude. The precipitation gradient of $\delta^{18}O$ is from −0.15–0.5‰/100 m with values in the range of the middle altitude European mountains of 0.2–0.3‰ (Clark and Fritz, 1997). The sample from the Hranicka Abyss (HA) falls between river water and the carbonate aquifer water, possibly indicating equal proportions of water from both sources or a significant proportion of lower altitude precipitation. The sample from the B Cave (BC) is close to the carbonate aquifer water and the sample from Death Cave (DC) is closer to the river water. However, this sample is located far from the river and has increased concentration of nitrate with a low EC value (Table 1), suggesting mixing with shallow groundwater contaminated by agriculture activities.

In Fig. 5, the sample from the river is isotopically depleted compared to other points and has a much lower concentration of bicarbonate. However, other samples have extremely enriched values of $\delta^{13}C$ between 0 and -2‰ and their bicarbonate concentrations are the highest in samples from the carbonate aquifer and the B-cave. Samples from the Hranicka Abyss and from Death Cave have lower bicarbonate values, probably caused by de-gassing, but still contain high $\delta^{13}C$

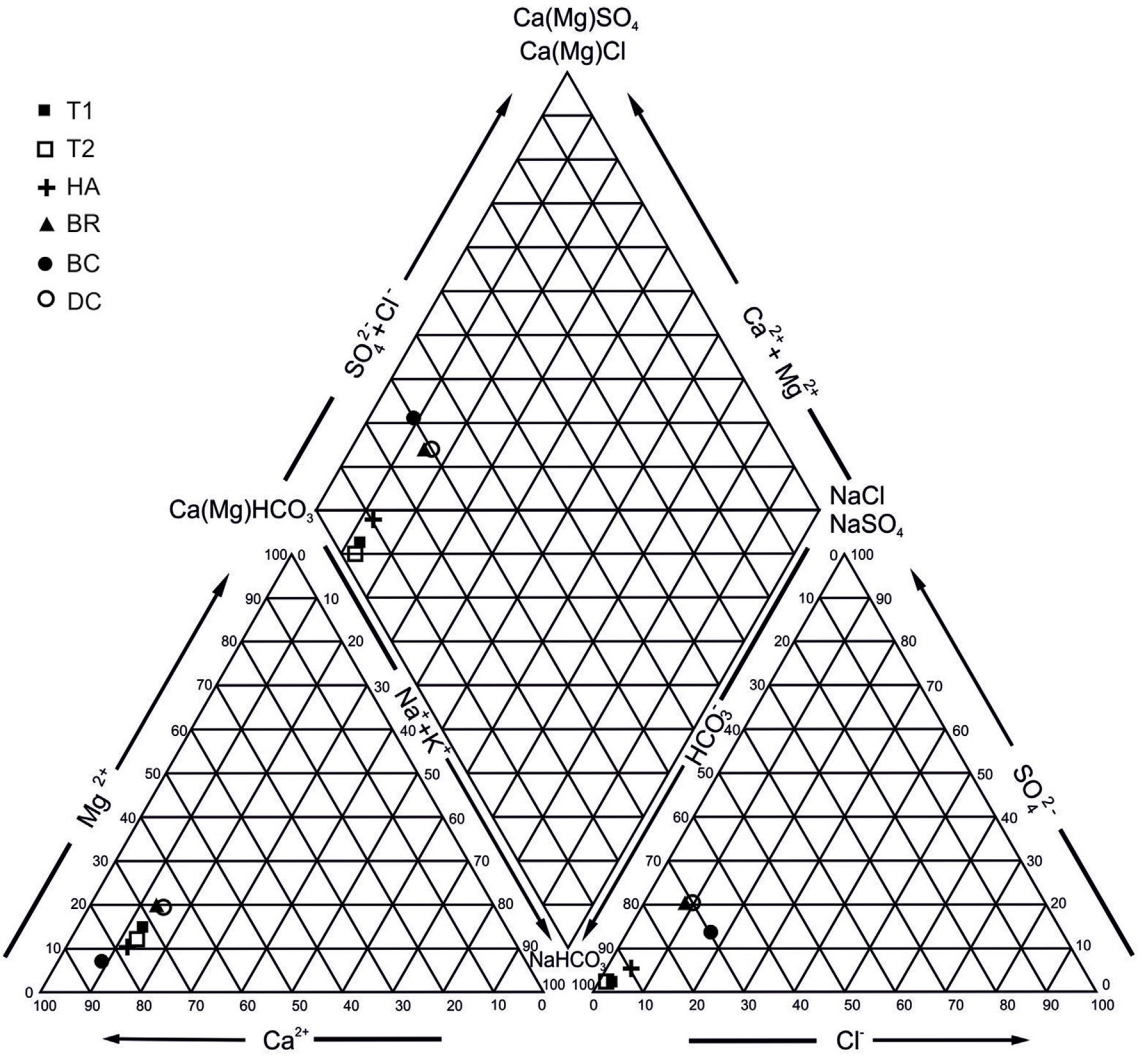

Fig. 3. Piper diagram for representative water samples from pumping wells (T1, T2), abyss (HA), caves (BC, DC), and river (BR) from May 2017.

Table 2
Isotopic data.

Sample/isotope	T1	T2	HA	River	BC	DC
δ^2H [‰] 2016	−71.1	−71.3	–	−66.2	–	–
δ^2H [‰] 2018	−71.9	−72	−70.9	−68	−71.7	−70.6
δ2H [‰] 2018				−70.63		
δ^{18}O [‰] 2016	−10.3	−10.1	–	−9.7	–	–
δ^{18}O [‰] 2017	−10.1	−10	−9.9	−9.6	−10.1	−9.8
δ^{18}O [‰] 2018				−9.94		
δ^{13}C(DIC) [‰] 2016	−0.25	−0.18	–	−18.77	–	–
δ^{13}C(DIC) [‰] 2017	−1.24	−1.05	−1.86	−15.15	−0.64	−0.91
δ^{34}S [‰] 2017	–	−2.7	−4.5	−2.6	−1	−1.8
Tritium [TU] 2017	2.9	3.2	2.1	8.7	1.2	2.9

values.

Values of $\delta^{34}S(SO_4)$ vs. sulfate concentrations are shown in Fig. 6. Samples from the river (RB) and carbonate aquifer (T2) have similar $\delta^{34}S(SO_4)$ values and sulfate concentrations, suggesting the same origin of sulfate. The most probable source of sulfate is atmospheric deposition from industrial sources of contamination in northern Moravia with $\delta^{34}S(SO_2)$ values between −2.5 and −3‰ (Buzek et al., 2017). Only a small fractionation was seen between SO_2 and SO_4 and values for sulfate are close to those for their atmospheric source Clark and Fritz, 1997). Samples from Death Cave (DC) and the Hranice Abyss (HA) have more negative values around −4.0‰ and higher sulfate concentrations

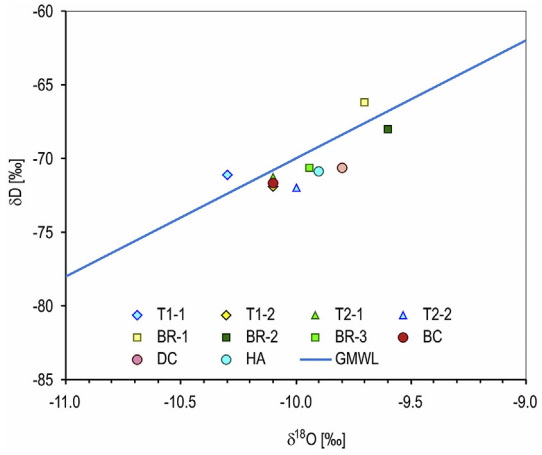

Fig. 4. Data for δ^2H and δ^{18}O.

of about 69 mg/l. The DC sample also has an increased nitrate concentration (Table 1) and seems to be affected by agricultural contamination.

Tritium activity of 8.7 TU in the river is within the range from 4 TU to 10 TU reported for precipitation in Czech Republic (Jankovec et al., 2017). Tritium activities in the carbonate aquifer are 2.9 and 3.2 TU, in

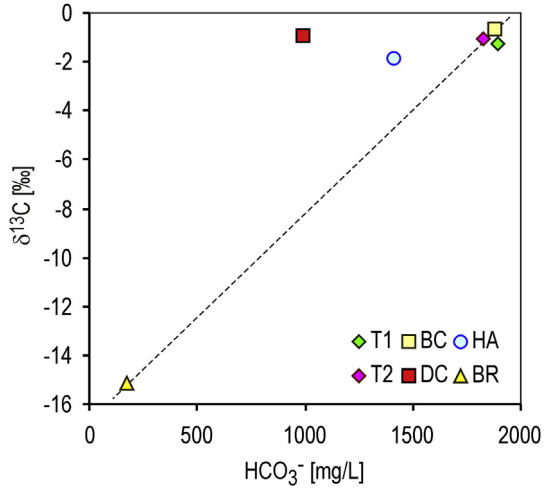

Fig. 5. Values of $\delta^{13}C$ vs HCO_3.

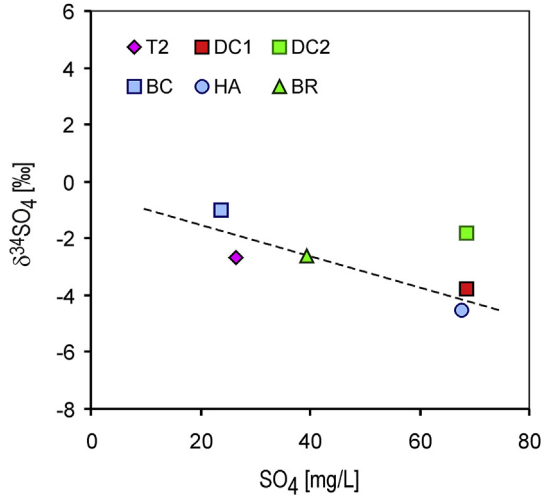

Fig. 6. Values of $\delta^{34}S(SO_4)$ vs. sulfate concentration.

the abyss 2.1 TU, and in Death Cave and B Cave 2.9 and 1.2 TU, respectively (Table 2). If a river water activity of 8.7 TU is considered as activity of recharged groundwater, the age of samples would be about 20 years. However, groundwater in the soil profile above the aquifer probably infiltrated earlier and the values in the carbonate aquifer indicate a minimum age which is somewhere between 20 and 50 years (tritium detection limit as indicated by Clark and Fritz, 1997). Surprisingly, tritium activity in B Cave is lower compared to deep carbonate aquifer, indicating an older water component. However, wells in the carbonate aquifer are pumped and thus could be partly recharged by younger water from their depression cones.

4.4. Speciation modeling

Selected results of speciation modeling are provided in Table 3.

All samples are supersaturated with respect to calcite and aragonite. Supersaturation with respect to dolomite is not reached in the sample from the Hranice Abyss (HA) and again in the DC sample. All samples are undersaturated with respect to gypsum. Several samples, especially T1 and T2 from the carbonate aquifer, are supersaturated with respect to fluorite. All samples are undersaturated with respect to Mg-minerals: magnezite, talc, and huntite (values not shown). In contrast, samples are supersaturated with respect to quartz. The most striking feature is extremely high values of log P_{CO2}, reaching −0.11 in the samples from the carbonate aquifer. The HA sample from the surface lake of the abyss

Table 3
Selected results of speciation modeling.

Sample/parameter	T1	T2	HA	River	BC	DC
SI aragonite	**0.39**	**0.33**	**0.10**	**0.72**	**0.50**	**0.27**
SI calcite	**0.54**	**0.48**	**0.25**	**0.87**	**0.64**	**0.41**
SI dolomite	**0.49**	**0.29**	−0.31	**1.15**	**0.63**	−0.05
SI magnezite	**−1.17**	**−1.27**	−1.45	−1.23	**−1.06**	−1.56
SI talc	−7.69	−8.16	−9.75	−5.11	−7.30	−7.67
SI fluorite	**0.13**	**0.18**	−0.12	−2.54	**0.24**	−0.96
SI gypsum	−1.84	−1.78	−1.36	−2.02	−1.82	−1.36
SI quartz	**0.21**	**0.28**	**0.19**	−0.55	**0.27**	**0.12**
Log P_{CO2}	−0.11	−0.11	−0.23	−3.34	−0.27	−0.65
Total C [mmol/l]	57.76	58.26	48.29	2.758	51.24	24.06

Bold-supersaturation.

is influenced by de-gassing, but its log P_{CO2} value is still −0.23. In contrast, sample BR from the river is almost at equilibrium with atmospheric P_{CO2}. Values of total C in the carbonate aquifer are about 20 times higher than in the river, with a maximum of 58.26 mmol/l in the sample from well T2.

5. Discussion

There are at least two pieces of evidence suggesting a deep mantle origin of CO_2. First, values of $\delta^{13}C$ for the carbonate aquifer and karst water samples are highly enriched, in the range from −0.25 to −1.05‰. In contrast, surface water in the Bečva River has values in the range from −15.15 to −18.77‰ depending on the season, which is in good agreement with values expected for an open CO_2 system after reaction with carbonates (Clark and Fritz, 1997). Highly enriched $\delta^{13}C$ values are even higher than those in the Eger Rift in western Bohemia (Dupalova et al., 2012; Noseck et al., 2009), where the input of mantle CO_2 has been proven (Weinlich et al., 1999). High inputs of hypogenic CO_2 are also consistent with very high calculated log P_{CO2} values (Table 3), which are much higher compared to the values typical for CO_2 from the epikarst zone (Faimon et al., 2012; Pracný et al., 2016a, 2016b).

Helium isotopes are used in groundwater studies to constrain groundwater age and origin (Phillips and Castro, 2003; Plummer et al., 2012). Isotopes of helium dissolved in the water of the Hranicka Abyss provide another piece of evidence for mantle origin of gases. Here we present a brief summary of data from the literature (Meyberg and Rinne, 1995). In this research, samples were taken by speleo-divers at a depth of about 40 m. The $^3He/^4He$ ratios were 4.5×10^{-6}, with a resulting R/R_a ratio = 3.2 where R_a is an atmospheric value of 1.4×10^{-6}. The R/R_a value is similar to values of mantle-derived helium in springs of central Italy (Minissale, 2004). Assuming a value of 1–3 x 10^{-5} for mantle helium isotopes, the mantle helium input would be 15–45% (average 30%). Concentrations of total dissolved helium were from 6.915×10^{-6} to 2.074×10^{-5} cm^3 STP/cm^3, i.e., which is 150–450 times higher than the concentration of helium dissolved in water in contact with air at a given temperature. Contamination by atmospheric gases dissolved in groundwater at shallow depth is also possible (Clark, 2015). However, the $^{20}Ne/^4He$ value of 6×10^{-3} was much lower than the atmospheric value of 4, thus excluding the impact of mixing with waters equilibrated with the air.

The origin of water in the Hranice Karst is more problematic and is less constrained than the origin of dissolved gases. Potential sources are the Bečva River, recharge directly on karst or inflow from non-karstic rocks. Results of a Hierarchical Cluster Analysis (HCA) for water samples are shown in Fig. 7. Samples from the deep carbonate aquifer (T1 and T2), B Cave (BC) and the Hranicka Abyss (HA) lie in the same cluster, which suggests the same origin. Sample from the river (BR) is partly linked to Death Cave (DC) sample, also suggesting similar composition. This is supported by the Piper diagram (Fig. 3), in which both the river (BR) and Death Cave (DC) samples are located close to each

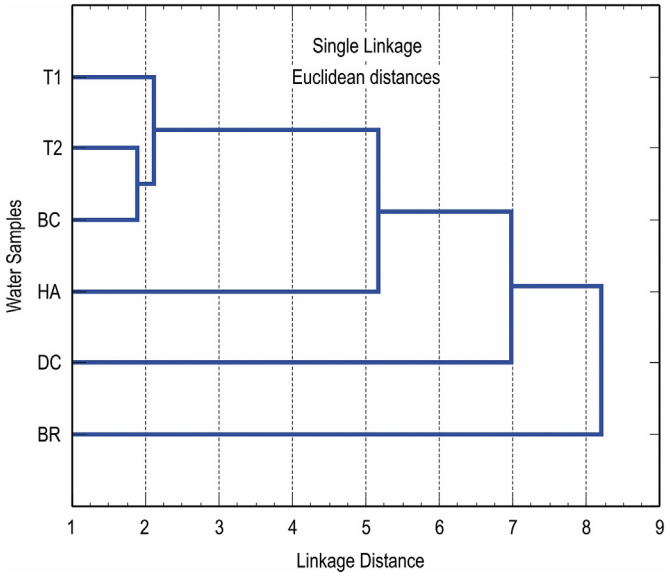

Fig. 7. Results of Hierarchical Cluster Analysis (HCA) of water sample data based on principal ions and trace elements.

other. However, the river water probably represents groundwater from the shallow aquifer connected to the river. Furthermore, the DC water seems to be influenced by agriculture contamination as indicated by high nitrate concentrations. Another piece of evidence is based on isotopic $\delta^{18}O$ data (Fig. 4), where T1 and T2 samples in the carbonate aquifer are depleted by 0.5–0.6‰ compared to the river, suggesting, under the assumption of a precipitation gradient of 0.2–0.3‰/100 m for $\delta^{18}O$ (Clark and Fritz), that the recharge zone should be situated at altitude about 160–200 m higher than the river valley. The precipitation altitude isotopic gradient is generally lower in warmer low-relief regions (Squeo et al., 2006; Clark, 2015) and the value of 0.2‰ seems to be reasonable for the moderate hilly region of central Moravia. Isotopic composition of the river water is generally similar all year around, and recharge of isotopically more depleted river water in late winter is not likely. Water samples from the Hranicka Abyss (HA) show a significant river water component.

Inverse geochemical modeling has been performed with the PHREEQC code to evaluate potential scenarios of aquifer water chemistry formation. Initial water composition was lacking because no data for shallow groundwater above the river valley were available. For this reason, water chemistry in the river was used because the river in the period without rain is supplied by groundwater, which represents a shallow groundwater chemical composition. The final water composition was groundwater from the carbonate aquifer in well T1. The models were calibrated using $\delta^{13}C$(DIC) data in well T1, i.e., −0.25‰. The initial $\delta^{13}C$ values were set to +4.0‰ for carbonates (consistent with unpublished data of 4.2‰, M. Geršl) and −1‰ for endogenous CO_2, respectively. These values resulted in the best convergence of models. Modeling results are shown in Table 4.

5.1. Model 1

In this model, Mg-rich calcite with composition $Ca_{0.86}Mg_{0.14}CO_3$ was used. Any lower value of Mg resulted in convergence problems. Halite and sylvite (KCl) were used to provide Cl- and corresponding anions. Sulfate was ignored because its concentration changes were relatively small and saturation indices for gypsum were negative (Table 3). The model suggested dissolution of 9.888 mmol/l of Mg-calcite and the input of a large amount of CO_2, 29.7 mmol/l. Dissolution of trace amounts of halite and sylvite was also suggested, being 0.655 mmol/l and 0.028 mmol/l, respectively. Also, removal of 0.378 mmol/l Mg by cation exchange and input of 0.757 mmol/l of exchangeable Na was also predicted. Although the model could reproduce the formation of groundwater in the carbonate aquifer, the Mg content in calcite was too high. Data for carbonate rocks at this site were much lower (Zimák and Štecl, 2004). However, it is possible that carbonates with higher Mg contents are present locally because available data are based on only a few samples collected in caves. Also, the dissolution of Mg-carbonates is frequently non-stoichiometric and Mg is preferentially enriched in solution (Pracny et al., 2017). Furthermore, for an estimated bulk solids density of 2.0 kg/dm^3 and a porosity of 0.10, 1 L of water is in contact with 20 kg of solids, or more than 200 mol of Mg-calcite, i.e., a large reservoir is available for dissolution. Porosities of the carbonate matrix, where water acquires its composition, are probably even lower.

5.2. Model 2

In the second modeling scenario, Mg-silicate talc was used as an additional potential source of Mg. This mineral dissolves congruently (Drever, 1997). Aluminosilicates such as biotite could be also used, but they dissolve incongruently and formation of secondary minerals, e.g., kaolinite has to be taken into account. In this model, a much lower content of Mg in calcite is needed with the resulting formula of $Ca_{0.985}Mg_{0.015}CO_3$. Compared to the previous model, precipitation of quartz is allowed. The suggested amount of dissolving Mg-calcite is lower, equalling 7.509 mmol/l, but there is a slightly higher input of CO_2 equalling 30.63 mmol/l. Approximately 0.716 mmol/l of talc dissolves and 2.715 mmol/l of quartz precipitates. The amount of dissolved sylvite is 0.588 mmol/l. Again, there is a removal of 0.894 mmol/l of Mg and 0.43 mmol/l of K, and an input of 2.218 mmol/l of Na by cation exchange. Both models can reproduce formation of the carbonate aquifer groundwater, but the second model gives more realistic contents of Mg in the carbonates.

Based on the similarity of water chemistries, a hypothesis of water mixing was tested. A simple mixing model was proposed for two end-members: (1) “mature” carbonate aquifer water, T_{mean}, produced by interaction of endogenous CO_2 with carbonate matrix and represented by average water from wells T1 and T2, and (2) shallow aquifer water, represented by river water, BR, which has a similar chemistry to the shallow aquifer water (compare position of Death Cave water and river water in Figs. 3 and 7):

$$RM = b_1 T_{mean} + (1 - b_1)BR \quad (1)$$

where RM is the resulting mix and b_1 is the mixing parameter.

RM, T_{mean}, and SW represent vectors of compositions. The ratio $b_1/(1\text{-}b_1)$ gives the resulting mixing ratio.

The parameter b_1 was determined by regression analysis. For the analysis, only the cumulative components were applied, i.e., species values and concentrations, EC, total C, δ^2H, and $\delta^{18}O$. The results of the

Table 4
Transfer of phases resulting from the inverse geochemical modeling (in mmol/l).

Model	Mg-calcite	CO_2(g)	Talc	SiO_2	Halite	Sylvite	MgX2	NaX	KX
Model 1	+9.888	+29.7	–	–	+0.655	+0.028	−0.378	+0.757	–
Model 2	+7.509	+30.63	+0.716	−2.715	–	+0.588	−0.894	+2.218	−0.430

+ dissolution, - precipitation, X – cation exchanger.

Table 5
Regression models with the parameter b_1 ($\alpha = 0.05$).

Model	b_1 estimate	Standard error	t-value	p-value	Lo. Conf	Up. Conf
HA = f(T_{mean}, BR)	0.638	0.022	29.38	0.000	0.594	0.683
BC = f(T_{mean}, BR)	0.991	0.007	152.40	0.000	0.978	1.004
DC = f(T_{mean}, BR)	0.152	0.018	8.47	0.000	0.115	0.189

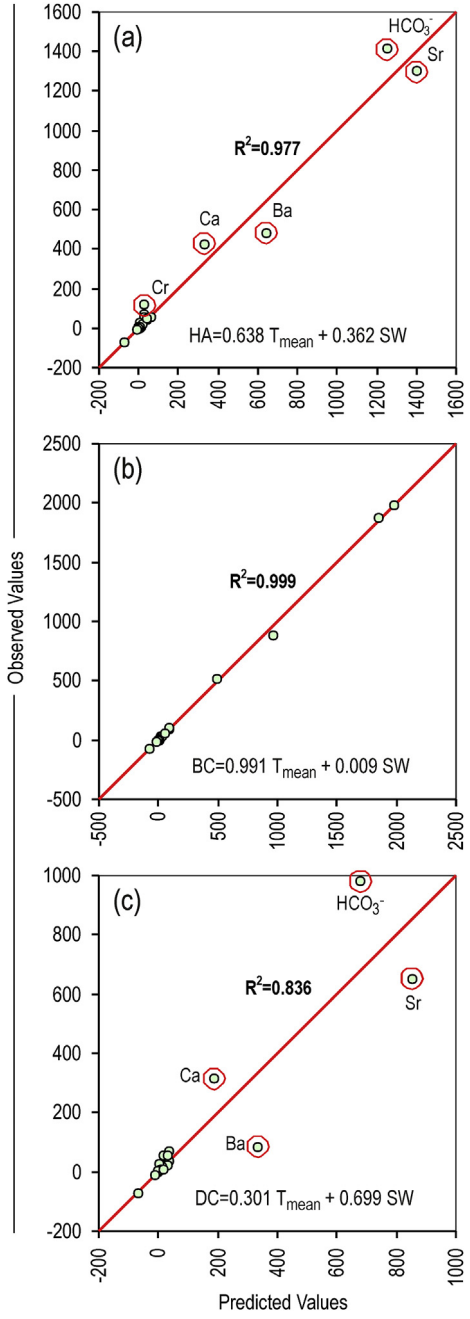

Fig. 8. Mixing models – regression results of deep aquifer groundwater T_{mean} and shallow groundwater SW. (a) Water HA, (b) water BC (c); water DC.

regression analysis are in Table 5 and Fig. 8.

All calculated parameters b_1 and models (Table 5) are statistically significant at $\alpha = 0.05$. The best model fit was observed for B Cave, BC = 0.991 T_{mean} + 0.009 BR (Fig. 8b) as indicated by $R^2 = 0.999$. In fact, the share of BR water in this sample is minimal and the BC water is dominated by the deep aquifer water.

The model HA = 0.638 T_{mean} + 0.362 BR (Fig. 8a) for Hranicka Abyss is somewhat worse ($R^2 = 0.977$). It shows some deviations for minor aqueous components (Cr, Ba, Sr) and also for major components (Ca, HCO_3^-) that might be due to post-mixing processes. The model is justified by the accessibility of runoff from the slope adjacent to the abyss and observed hydraulic connection between the river and the abyss.

The model DC = 0.152 T_{mean} + 0.848 BR (Fig. 8c) for Death Cave is the worst ($R^2 = 0.906$) although still of a high statistical significance. This is the result of two larger deviations of Ca and Ba concentrations. The enhanced Ca concentrations can be caused by mixing with water from another source not accounted for in the mixing models. The water is affected by contamination and has high nitrate concentration. The models express the share of shallow water in the actual mineral water composition.

The conceptual model of the studied aquifer is shown in Fig. 9. The greatest fraction of water infiltrates at the elevated uplands at altitudes of about 160–200 m higher than the river valley as indicated by depleted δ^2H and $\delta^{18}O$ values. A part of the water is probably recharged in non-karstic regions, but it cannot be quantified due to the lack of water chemistry data from non-carbonate rocks. The water then descends and warms up. During its migration, the water acquires high concentrations of dissolved CO_2 with $\delta^{13}C$ values of about −1‰ and dissolves Mg-rich carbonates and silicates. The karstification already starts at depth and when the water ascends, it cools down and becomes more aggressive towards carbonates, widening the pre-existing conduits created by tectonic processes. Flow directions are generally towards the river, but can be reversed during high water level periods in the river. Extremely high dissolved concentrations of CO_2 (log P_{CO2} up to −0.11, Table 3) result in two-phase flow which increases water levels in the caves and in the abyss. In the Hranicka Abyss, the water chemistry is affected by mixing of deep water with the water recharged at the eastern slope of the abyss and from the river. Some degree of mixing with water from the river and possibly also from the shallow aquifer is observed in samples from caves, especially from Death Cave.

Several stages of karstification were identified at the study site (Otava, 2005). The initial karstification with the development of mogote-type karst probably already occurred in late Paleozoikum and continued until Miocene transgression, when the region was covered by a thick layer of clastic sediments. During this period, there was limited recharge across confining units and buoyancy-driven flow probably occurred, similar to the initial stages of the Buda Thermal Karst formation (Havril et al., 2016). The erosion of the confining units and incision of the Bečva River valley resulted in gravity-driven circulation and cooling of ascending groundwater with resulting enlargement of pre-existent tectonic features by dissolution (Andre and Rajaram, 2004; Sandeep et al., 2016). Currently the dissolution can be enhanced by mixing with river water during extreme flood events. The role of fluids is consistent with their role in development of several other hypogenic caves in the world as summarized by Klimchouk (2009) such as Wind Cave in Black Hills in South Dakota, USA, and Lechuguilla Cave in New Mexico, USA.

6. Conclusions

Fluid origins in the Hranice Karst can only be partly constrained. The conceptual model indicates that at least a part of the CO_2 gas originates in the mantle as indicated by very enriched $\delta^{13}C$(DIC) values

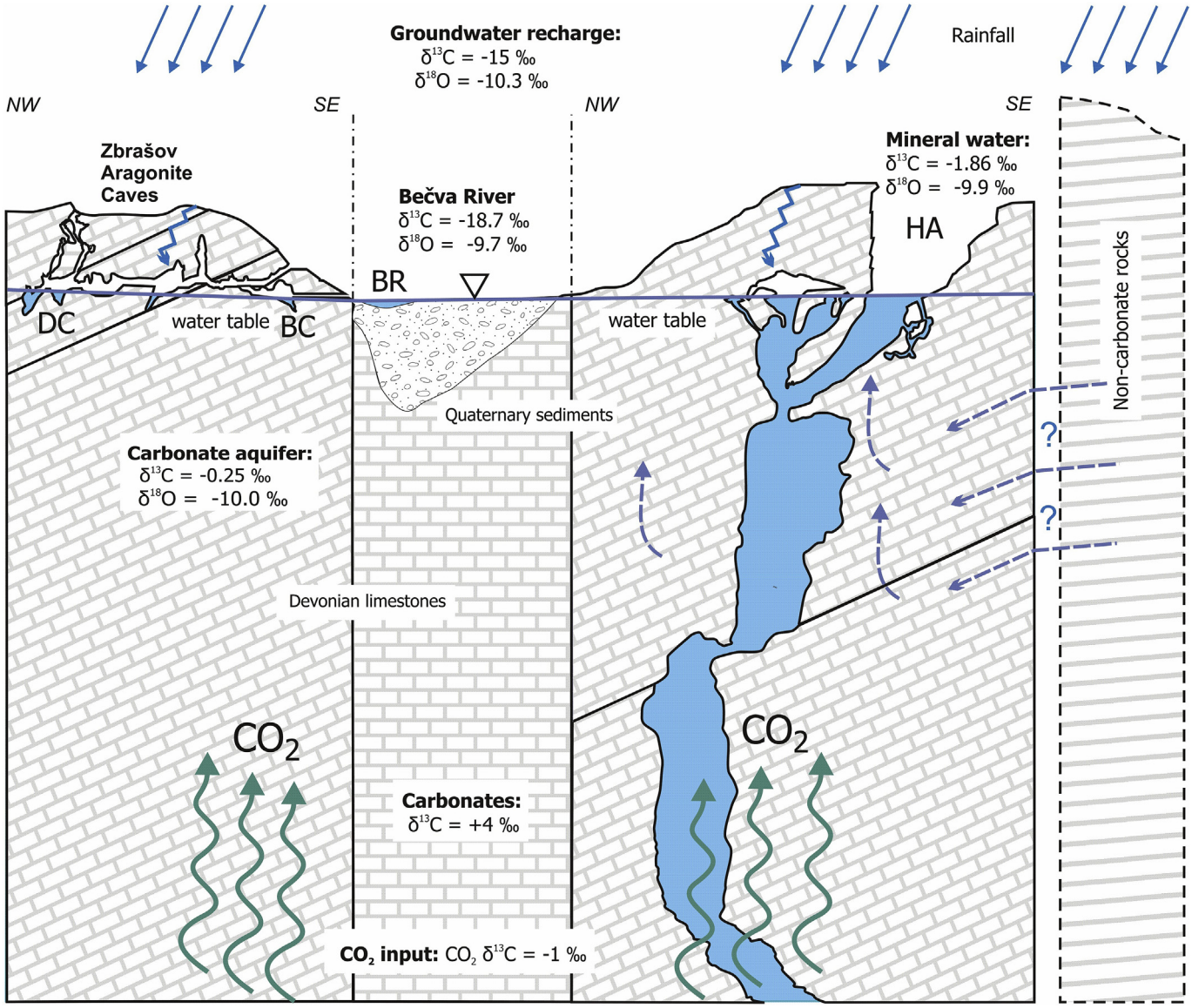

Fig. 9. Conceptual model of water and gas fluxes indicated by arrows in the Hranice Karst, representative isotopic data are included.

and He isotope values from the literature. The origin of groundwater in the karstic aquifer exploited in the Teplice nad Bečvou Spa is meteoric with a recharge area in the uplands about 200 m above the Bečva River valley as indicated by depleted values of δ^2H and $\delta^{18}O$ compared to the river water. Based on detectable tritium, the groundwater is from 20 to 50 years old. Water in the Hranicka Abyss and in the Zbrašovské Aragonitové Caves is a mixture of carbonate aquifer groundwater with the river water with variable amounts of both components. Water in Death Cave Lake is probably affected by shallow groundwater recharge contaminated by agricultural activities. Inverse geochemical modeling suggested reaction of Mg-rich calcite with very high amount of deep CO_2 (about 30 mmol/l) plus dissolution of trace amounts of halite and sylvite and cation exchange. Another possible scenario includes Mg-depleted calcite and a Mg-silicate (talc) as a source of Mg. Both scenarios were calibrated using $\delta^{13}C$(DIC) values and gave satisfactory results. A conceptual model of the site has been developed which includes a gravity-driven flow system, (Tóth, 1999), where recharged meteoric water is heated at depth and acquires large amounts of hypogenic CO_2. The water cools down during its ascent, becomes more undersaturated with respect to calcite and has created karst features such as the Zbrašovské Aragonitové Caves and the Hranicka Abyss. The Hranice Karst is an example of a multi-stage development system in which flow conditions were changing along with the presence or absence of confining units. The Miocene transgression and later incision of the Bečva River Valley played an important role in the development of flow patterns and, thus, in the formation of water chemistry.

Acknowledgements

We thank Barbora Šimečková from the Zbrašovské Aragonitové Caves for encouragement and permission for sampling in the caves and Jiří Zimák from Palacky University who provided us with his data about composition of limestones from the Hranice Karst. We also thank František Buzek from the Czech Geological Survey for isotopic analyses and discussion about isotopes and Martin Mihaljevič from Charles University for water chemistry analyses. Finally, we thank executive editor Michael Kersten, associate editor François Chabaux and especially two anonymous reviewers who helped to improve this manuscript.

References

Aitchison, J., 1986. The Statistical Analysis of Compositional Data. Chapman and Hall, London, UK 1986.

Andre, B.J., Rajaram, H., 2004. Dissolution of limestone fractures by cooling waters: early development of hypogene karst systems. Water Resour. Res. 41 (1), W01015. https://doi.org/10.1029/2004WR003331.

Audra, P., Palmer, A.N., 2015. Research frontiers in speleogenesis. Dominant processes, hydrogeological conditions and resulting cave patterns. Acta Carsol. 44 (3), 315–348. https://doi.org/10.3986/ac.v44i3.1960.

Bajjali, W., Clark, I.D., Fritz, P., 1997. The artesian thermal groundwater of northern Jordan: insights into their recharge history and age. J. Hydrol. 192 (1–4), 355–382. https://doi.org/10.1016/S0022-1694(96)03082-X.

Bábek, O., Briestenský, M., Přecechtělová, G., Štěpančíková, P., Hellstrom, J.C., Drysdale, R.N., 2015. Pleistocene speleothem fracturing in the foreland of the Western Carpathians: a case study from the seismically active eastern margin of the Bohemian Massif. Geol. Q. 59, 491–506. https://doi.org/10.7306/gq.1225.

Bunta, J.K., 2015. Hranice Abyss - World's Second Deepest Known Underwater Cave. Online: http://www.boinc.sk/clanky/hranice-abyss-worlds-second-deepest-known-underwater-cave Visited: May 2018.

Buzek, F., Cejkova, B., Hellebrandova, L., Jackova, I., Lollek, V., Lnenickova, Z., Matalakova, R., Veselovsky, F., 2017. Isotope composition of NH_3, NO_x and SO_2 air pollution in the Moravian-Silesian region, Czech Republic. Atmos. Pollut. Res. 8, 221–232. https://doi.org/10.1016/j.apr.2016.08.011.

Caramana, G., 2002. Exploring on of the world's deepest sinkholes: the Pozzo del Merro (Italy). In: Underwater Speleology, February, pp. 4–8.

Clark, I., 2015. Groundwater, Geochemistry and Isotopes. CRC Press, Taylor & Francis Group, pp. 438.

Clark, I., Fritz, P., 1997. Environmental Isotopes in Hydrogeology. Lewis Publishers, pp. 328.

Čížek, P., Tomek, C., 1991. Large-Scale thin-skinned tectonics in the eastern boundary of the Bohemian Massif. Tectonics 10, 273–286.

Davies, J.C., 2002. Statistics and Data Analysis in Geology, third ed. John Wiley & Sons, New York.

Dlešťík, P., Bábek, O., 2013. Shallow geophysical mapping of buried karst surface near hranice using electrical resistivity tomography (In Czech). Geologické výzkumy na Moravě a ve Slezsku 2013, 174–177.

Drever, J.I., 1997. The Geochemistry of Natural Waters, Surface and Groundwater Environments, third ed. Prentice Hall.

Dupalová, T., Sracek, O., Vencelides, Z., Žák, K., 2012. The origin of thermal waters in the northeastern part of the Eger Rift, Czech Republic. Appl. Geochem. 27 (3), 689–702. https://doi.org/10.1016/j.apgeochem.2011.11.016.

Dvořák, J., Friáková, O., 1978. Stratigraphy of the Palaeozoic near Hranice na Morave. Czech Geological Survey report 18. pp. 1–50.

Filzmoser, P., Hron, K., Reimann, C., 2009. Principal component analysis for compositional data with outliers. Environmetrics 20, 621–632.

Faimon, J., Ličbinská, M., Zajíček, P., Sracek, O., 2012. Partial pressures of CO_2 in epikarstic zone deduced from hydrogeochemistry of permanent drips, the Moravian Karst, Czech Republic. Acta Carsol. 41 (1), 47–57. https://doi.org/10.3986/ac.v41i1.47.

Gary, M., Sharp, J.M., 2006. Volcanogenic karstification of Sistema Zacatón, Mexico. Geol. Soc. Am. Spec. Pap. 404, 79–89.

Geršl, M., 2016. Discrimination of the Hranice Karst waters on the basis of archive analyses (In Czech). In: Geoscience Research Reports 49. pp. 247–252.

Goldscheider, N., Mádl-Szönyi, J., Erőss, A., Schill, E., 2010. Review: thermal water resources in carbonate rock aquifers. Hydrogeol. J. 18, 1303–1318. https://doi.org/10.1007/s10040-010-0611-3.

Guterch, B., Lewandowska-Marciniak, H., 2002. Seismicity and seismic hazard in Poland. Folia Quat. 73, 85–99.

Hartley, A.J., Otava, J., 2001. Sediment provenance and dispersal in a deep marine foreland basin: the Lower Carboniferous Culm Basin, Czech Republic. J. Geol. Soc. 158, 137–150. https://doi.org/10.1144/jgs.158.1.137.

Havril, T., Molson, J.W., Mádl-Szőnyi, J., 2016. Evolution of fluid flow and heat distribution over geological time scales at the margin of unconfined and confined carbonate sequences – a numerical investigation based on the Buda Thermal Karst analogue. Mar. Petrol. Geol. 78, 738–749. https://doi.org/10.1016/j.marpetgeo.2016.10.001.

Holcova, K., Hrabovsky, J., Nehyba, S., Hladilova, S., Dolakova, N., Demeny, A., 2015. The Langhian (middle Badenian) carbonate production event in the moravian part of the Carpathian Foredeep (central Paratethys): a multiproxy record. Facies 61, 419.

Jankovec, J., Vitvar, T., Šanda, M., Matsumoto, T., Han, L.-F., 2017. Groundwater recharge and residence times evaluated by isotopes of hydrogen and oxygen, noble gases and CFCs in mountain catchment in the Jizera Mts., northern Czech Republic. Geochem. J. 51, 423–437. https://doi.org/10.2343/geochemj.2.0469.

Kalvoda, J., Bábek, O., Fatka, O., Leichmann, J., Melichar, R., Nehyba, S., Špaček, P., 2008. Brunovistulian terrane (Bohemian Massif, central Europe) from late Proterozoic to late Paleozoic: a review. Int. J. Earth Sci. 97, 497–518. https://doi.org/10.1007/s00531-007-0183-1.

Klimchouk, A., 2009. Morphogenesis of hypogenic caves. Geomorphology 106, 100–117. https://doi.org/10.1016/j.geomorph.2008.09.013.

Klimchouk, A., Auler, A.S., Bezerra, F.H.R., Cazarin, C.L., Balsamo, F., Dublyansky, Y., 2016. Hypogenic origin, geological controls and fuctional organization of a giant cave system in Precambrian carbonates, Brazil. Geomorphology 253, 385–405. https://doi.org/10.1016/j.geomorph.2015.11.002.

Kovac, M., Andreyeva-Grigorovich, A., Bajraktarevic, Z., Brzobohaty, R., Filipescu, S., Fodor, L., Harzhauser, M., Nagymarosy, A., Oszczypko, N., Pavelic, D., Rogl, F., Saftic, B., Sliva, L., Studencka, B., 2007. Badenian evolution of the Central Paratethys Sea: paleogeography, climate and eustatic sea-level changes. Geol. Carpathica 58, 579–606.

Mádl-Szönyi, J., Tóth, A., 2015. Basin-scale conceptual groundwater flow model for an unconfined and confined thick carbonate region. Hydrogeol. J. 23, 1359–1380. https://doi.org/10.1007/s10040-015-1274-x.

Meyberg, M., Rinne, B., 1995. Messung des $^3He/^4He$-Isotopen-verhältnisses in Hranicka Propast (Tschechische Republik) (Measurement of $^3He/^4He$ isotopic ratios in Hranicka Propast, (Czech Republic)). Die Höhle Z. Karst und Höhlenkunde 46 (1), 5–8.

Minissale, A., 2004. Origin, transport and discharge of CO_2 in central Italy. Earth Sci. Rev. 66 (1–2), 89–141. https://doi.org/10.1016/j.earscirev.2003.09.001.

Minissale, A., Vaselli, O., Tassi, F., Magro, G., Grechi, G.P., 2002. Fluid mixing in carbonate aquifers near Rapolano (central Italy) : chemical and isotopic constraints. Appl. Geochem. 17, 1329–1342. https://doi.org/10.1016/S0883-2927(02)00023-9.

Noseck, U., Rozanski, K., Dulinski, M., Havlová, V., Sracek, O., Brasser, T., Hercik, M., Buckau, G., 2009. Carbon chemistry and groundwater dynamics at natural analogue site Ruprechtov, Czech Republic: insights from environmental isotopes. Appl. Geochem. 24, 1765–1776. https://doi.org/10.1016/j.apgeochem.2009.05.007.

Novák, A., Bábek, O., Kapusta, J., 2017. Late quaternary tectonic switching of siliciclastic provenance in the strike-slip-dominated foreland of the western Carpathians; upper morava basin, Bohemian Massif. Sediment. Geol. 355, 58–74. https://doi.org/10.1016/j.sedgeo.2017.04.005.

Otava, J., 2005. Polycyclic origin of fossil karst at Hranice Paleozoic, Czech Republic. In: 14th International Congress of Speleology, Abstract Book 121-122, Athens, Greece.

Parkhurst, D.L., Appelo, C.A.J., 1999. Guide to PHREEQC (version 2)-A Computer Program for Speciation, Batch-reaction, One-Dimensional Transport, and Inverse Geochemical Calculations. Water-resources investigations Report 99-4259. U.S. Geological Survey.

Phillips, F.M., Castro, M.C., 2003. Groundwater dating and residence time measurements. In: In: Drever, J.I., Holland, H.D., Turekian, K.K. (Eds.), Treatise on Geochemistry, vol. 5. Elsevier, pp. 451–497.

Plummer, L.N., Eggleston, J.R., Andreasen, D.C., Raffensperger, J.P., Hunt, A.G., Casile, G.C., 2012. Old groundwaters in the parts of the upper Patapsco aquifer, Atlantic coastal plain, Maryland, USA: evidence from radiocarbon, chlorine-36 and helium-4. Hydrogeol. J. 20, 1269–1294. https://doi.org/10.1007/s10040-012-0871-1.

Pracný, P., Faimon, J., Vsiansky, D., Kabelka, L., 2017. Evolution of Mg/Ca ratios during limestone dissolution under epikarstic conditions. Aquat. Geochem. 23 (2), 119–139. https://doi.org/10.1007/s10498-017-9313-y.

Pracný, P., Faimon, J., Kabelka, L., Hebelka, J., 2016a. Variations of carbon dioxide in the air and dripwaters of Punkva caves (Moravian karst, Czech Republic). Carbonates Evaporites 31 (4), 375–386. https://doi.org/10.1007/s13146-015-0259-0.

Pracný, P., Faimon, J., Sracek, O., Kabelka, L., Hebelka, J., 2016b. Anomalous drip in Punkva Caves (Moravian Karst): relevant implications for paleoclimatic proxies. Hydrol. Process. 30, 1506–1520. https://doi.org/10.1002/hyp.10731.

Sandeep, V.R., Chaudhuri, A., Kelkar, S., 2016. Permeability and flow field evolution due to dissolution of calcite in 3-D porous rock under geothermal gradient and throughflow. Transport Porous Media 112, 39–52. https://doi.org/10.1007/s11242-016-0631-0.

Schulmann, K., Gayer, R., 2000. A model for a continental accretionary wedge developed by oblique collision: the NE Bohemian Massif. J. Geol. Soc. Lond. 157, 401–416. https://doi.org/10.1144/jgs.157.2.401.

Špaček, P., Bábek, O., Štěpančíková, P., Švancara, J., Pazdírková, J., Sedláček, J., 2015. The Nysa–Morava zone: an active tectonic domain with late Cenozoic sedimentary grabens in the western Carpathians' foreland (NE Bohemian Massif). Int. J. Earth Sci. 104, 963–990. https://doi.org/10.1007/s00531-014-1121-7.

Squeo, F.A., Aravena, R., Aquirre, E., Pollastri, A., Jorquera, C.B., Ehleringer, B.R., 2006. Groundwater dynamics in a coastal aquifer in north-central Chile: implications for groundwater recharge in an arid ecosystems. J. Arid Environ. 67, 240–254. https://doi.org/10.1016/j.jaridenv.2006.02.012.

Tóth, J., 1999. Groundwater as a geologic agent: an overview of the causes, processes, and manifestations. Hydrogeol. J. 7, 1–14. https://doi.org/10.1007/s100400050176.

Tyráček, J., 1962. Fossil cockpit karst near Hranice na Moravě. Časopis pro Mineral. a Geol. 2, 176–181 (In Czech).

Ulrych, J., Ackerman, L., Balogh, K., Hegner, E., Jelínek, E., Pécskay, Z., Přichystal, A., Upton, B.G.J., Zimák, J., Foltýnová, R., 2013. Plio-Pleistocene basanitic and melilititic series of the Bohemian Massif: K–Ar ages, major/trace element and Sr–Nd isotopic data. Chem. Erde 73, 429–450. https://doi.org/10.1016/j.chemer.2013.02.001.

Weinlich, F.H., Bräuer, K., Kämpf, H., Strauch, G., Tesar, J., Weise, S.M., 1999. An active subcontinental mantle volatile system in the western Eger rift, Central Europe: gas flux, isotopic (He, C, and N) and compositional fingerprints. Geochem. Cosmochim. Acta 61 3563–3671. https://doi.org/10.1016/S0016-7037(99)00187-8.

Zimák, J., Štelcl, J., 2004. Natural Radioactivity of the Rock Environment in the Caves in Czech Republic (In Czech with English Summary). Palacky University Press.